

# Threshold Implementations of GIFT: A Trade-off Analysis

Naina Gupta, Arpan Jati, Anupam Chattopadhyay, Somitra Kumar Sanadhya, and Donghoon Chang

## Abstract

Threshold Implementation (TI) is one of the most widely used countermeasure for side channel attacks. Over the years several TI techniques have been proposed for randomizing cipher execution using different variations of secret-sharing and implementation techniques. For instance, Direct Sharing (4-shares) is the most straightforward implementation of the threshold countermeasure. But, its usage is limited due to its high area requirements. On the other hand, sharing using decomposition (3-shares) countermeasure for cubic non-linear functions significantly reduces area and complexity in comparison to 4-shares.

Nowadays, security of ciphers using a side channel countermeasure is of utmost importance. This is due to the wide range of security critical applications from smart cards, battery operated IoT devices, to accelerated crypto-processors. Such applications have different requirements (higher speed, energy efficiency, low latency, small area etc.) and hence need different implementation techniques. Although, many TI strategies and implementation techniques are known for different ciphers, there is no single study comparing these on a single cipher. Such a study would allow a fair comparison of the various methodologies. In this work, we present an in-depth analysis of the various ways in which TI can be implemented for a lightweight cipher. We chose GIFT for our analysis as it is currently one of the most energy-efficient lightweight ciphers. The experimental results show that different implementation techniques have distinct applications. For example, the 4-shares technique is good for applications demanding high throughput whereas 3-shares is suitable for constrained environments with less area and moderate throughput requirements. The techniques presented in the paper are also applicable to other blockciphers. For security evaluation, we performed *leakage assessment* on 3-shares (as it has good area versus speed trade-off) and combined 3-shares (as it uses a new implementation strategy). Experiments using 10 million traces show that the designs are protected against first-order attacks.

## Index Terms

Side-channel, Threshold Implementation, DPA, CPA, GIFT, TI

## I. INTRODUCTION

Implementing secure embedded systems has been a cat-and-mouse game since last few decades due to the constant development of side-channel attack techniques followed by new countermeasures. The security of even the smallest of embedded devices is of a major concern; as many of these devices have become an important part of our daily lives. The seminal work by Kocher et al. [1], [2] in the late 90's showed that unprotected cryptographic algorithms are vulnerable against side-channel attacks.

Over the years, many countermeasure techniques have been proposed to prevent such attacks, for instance introducing noise in the signal [3], to randomize intermediate values during computations i.e. masking [3], to balance the power consumption in circuit's design [4], etc. Despite these countermeasures, the devices are still vulnerable to some form of the side-channel attacks or the other; for example, masking still leaks some form of information in the presence of glitches [5], [6]. In 2006, Nikova et al. proposed a new countermeasure known as Threshold Implementation (TI) [7]. TI is based on secret-sharing and is secure even in the presence of glitches. TI soon became one of the most widely used countermeasures. As a result, there has been a lot of work in the past years towards developing new methodologies for secret-sharing and efficient implementation of TI. For example, in [8], the authors showed how to apply TI on the PRESENT cipher. Later, in 2013 Kutzner et al. [9] presented the *one S-box for all* technique to efficiently implement 3-shares. Furthermore, [10] describes how to speed-up search for the decomposed S-box and also derive the results for TI on all  $3 \times 3$  and  $4 \times 4$  S-boxes. Efficient TI implementation of AES is presented in [11]. However, the design exploration using all these TI methodologies and implementation techniques have not yet been performed for a single cipher on a common platform. In this work, we focus on performing such a detailed design analysis of TI using GIFT [12], which was introduced by Banik et. al. in CHES 2017.

*Our contributions.* First, we present a Correlation Power Analysis (CPA) [13] attack for an unprotected FPGA implementation of the GIFT cipher in § IV-A. Since a single round of GIFT uses 64-bit keys at a time and each S-box operation uses only 2-bits of the key, we implement the attack using 4 S-boxes at a time. In our experiments using Xilinx Kintex-7 FPGA, we are able to recover the secret key in less than 10,000 traces. Second, we implement multiple efficient TI countermeasures for GIFT. The implementations are protected against first-order power attacks. We support this claim by performing Test Vector Leakage Assessment methodology (TVLA) [14] using 10 Million real power traces on two of the protected implementations. These experiments are described in § IV-B. Third, we implemented nine different profiles using known TI techniques and provide

a trade-off analysis in terms of area, frequency, latency, power and energy. In particular, we focus on three TI techniques – 3-shares, combined 3-shares and 4-shares using various options. This analysis is presented in § III-B.

There are two common types of implementations for iterated block ciphers, namely the *serialized* and the *round-based*. The *serialized* implementations typically require significantly smaller area and have much reduced throughput; whereas the *round-based* implementations are much larger and have very high throughputs. In this work, we focused on high throughput implementations, so, we selected only the *round-based* implementations for our analysis.

The Boolean equations of any non-linear function (in our case S-box) are typically represented using Algebraic Normal Form (ANF). The implementation can directly be done using ANF, or it can be further minimized using a Boolean minimization tool like Espresso [15], [16], BOOM [17], ABC [18] etc. In our analysis, we found that logic minimization using Espresso and ABC leads to similar results in terms of overall area for GIFT. Whereas, a major difference was found between an implementation using ANF compared to the Boolean minimization tools. As a result, we present detailed analysis contrasting these two implementation methods. Further, many implementations skip the key-update masking, but it is possible that the *hamming weight* of certain parts of the key is leaked even for very simple key-schedules. Therefore, we considered the key-update masking in our analysis.

We implemented all the TI schemes and analyzed the synthesis results using the same library (TSMC 65nm Low Power). As discussed in § III-C, the 3-shares technique is 44.9% smaller but requires twice the number of clock cycles compared to the 4-shares technique. It is noteworthy to observe that both the designs have very similar overall energy requirements. Further, the combined 3-shares technique consumes the least amount of power, but the design requires a large number of clock cycles leading to a significantly low energy efficiency.

## II. PRELIMINARIES

### A. GIFT Specifications

GIFT is an SPN (substitution-permutation network) based cipher. Its design is strongly influenced by the cipher PRESENT [19]. It has two versions GIFT-64-128: 28 rounds with a block size of 64-bits and GIFT-128-128: 40 rounds with 128-bit blocks. Both the versions have 128-bit keys. For this work, we focus only on GIFT-128-128.

**Initialization.** The cipher state  $S$  is first initialized from the 128-bit plaintext represented as 32 nibbles of 4-bit represented as  $w_{31}, \dots, w_1, w_0$ . The 128-bit key is divided into 16-bit words  $k_7, k_6, \dots, k_0$  and is used to initialize the key register  $K$ .

**The Round Function.** Each round of the cipher comprises of a Substitution Layer (S-layer) followed by a Permutation Layer (P-layer) and a XOR with the round-key and predefined constants (AddRoundKey).

TABLE I  
GIFT S-BOX

$\mathbf{x}$	0	1	2	3	4	5	6	7	8	9	a	b	c	d	e	f
$\mathbf{S}(\mathbf{x})$	1	a	4	c	6	f	3	9	2	d	b	7	5	0	8	e

**S-layer (S):** Apply the same S-box to each of the 4-bit nibbles of the state  $S$ . The truth-table for the S-box is shown in Table I.

**P-layer (P):** This operation permutes the bits of the cipher state  $S$  from position  $i$  to  $P(i)$ . The permutation table is available in the design document [12] and we do not reproduce it here.

**AddRoundKey:** A 64-bit round key  $RK$  and a 7-bit round constant  $Rcon$  is XORed to a part of the cipher state  $S$  in this operation. The round key is extracted from the 128-bit key register  $K$  as  $RK = U||V$  where  $U \leftarrow k_5||k_4$  and  $V \leftarrow k_1||k_0$ . The round key  $U||V$  can be represented as  $= u_{31}, \dots, u_1, u_0 || v_{31}, \dots, v_1, v_0$ . The two halves of  $RK$ , namely,  $U$  and  $V$  are XORed to the cipher state as follows:  $b_{4i+2} \leftarrow b_{4i+2} \oplus u_i$  and  $b_{4i+1} \leftarrow b_{4i+1} \oplus v_i \forall i \in \{0, \dots, 31\}$ . The round constant  $(c_5 c_4 c_3 c_2 c_1 c_0)$  and a single-bit ‘1’ is XORed to the cipher state as defined below:

$b_{n-1} \leftarrow b_{n-1} \oplus 1$ ,  $b_{23} \leftarrow b_{23} \oplus c_5$ ,  $b_{19} \leftarrow b_{19} \oplus c_4$ ,  $b_{15} \leftarrow b_{15} \oplus c_3$ ,  $b_{11} \leftarrow b_{11} \oplus c_2$ ,  $b_7 \leftarrow b_7 \oplus c_1$  and  $b_3 \leftarrow b_3 \oplus c_0$ , where  $n - 1, 23, 19, 15, 11, 7$  and  $3$  denote bit positions in the cipher state respectively.

**Key Expansion and Constants Generation:** After AddRoundKey, the key register is updated as follows:  $k_7||k_6||\dots||k_1||k_0 \leftarrow k_1 \ggg 2||k_0 \ggg 12||\dots||k_3||k_2$ . The 6-bit round constant is initialized to zero and is updated before each round as  $(c_5, c_4, c_3, c_2, c_1, c_0) \leftarrow (c_4, c_3, c_2, c_1, c_0, c_5 \oplus c_4 \oplus 1)$ .

**GIFT Encryption.** As shown in Fig. 1, a single block is processed by the application of a series of round functions. At each round, S-layer, P-layer and AddRoundKey operations are performed on the previous cipher state. After 40 such rounds, the current state is provided as the ciphertext.



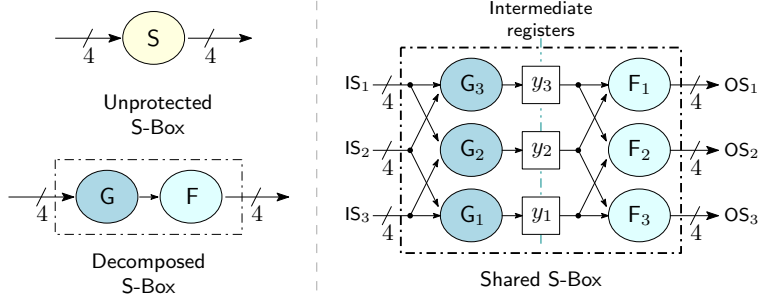


Fig. 2. Sharing using Decomposition (3-shares)

Following steps were implemented in order to compute the desired optimized quadratic Boolean functions for  $G$  and  $F$ :

- 1) For all possible combinations of the input to the functions  $g_i, f_i$  where  $i \in \{0, 1, 2, 3\}$ , compute its corresponding output from the ANF equations and check if its vectorial Boolean function [23] is balanced or not. If the combination is balanced, then add it to a set of possible coefficients for the ANF (say  $P$ ), otherwise discard it.
- 2) For each balanced coefficient in the set  $P$ , compute the corresponding  $G(X)$  iteratively.
- 3) Check whether this computed  $G(X)$  is a permutation or not. If yes, compute  $F(X)$  using  $S(G^{-1}(X))$ , otherwise discard this  $G(X)$ .
- 4) Check whether the computed  $F(X)$  is a quadratic function or not. If yes, add both the  $G(X)$  and  $F(X)$  functions to a set of possible decompositions, otherwise discard both of them. We obtained 80641 possible decompositions after this step.
- 5) Now considering the 15 possibilities of the constant term in the ANF, we obtained 1290241 total possible decompositions for GIFT S-box after filtering.
- 6) Keep only the  $G(X)$  and  $F(X)$  combinations which are permutations, discard the rest.
- 7) In order to choose the decomposition with minimum area, we applied the following two metrics:
  - For each of the possible decomposition, calculate the total ANF weight of  $G(X)$  and  $F(X)$  using the formula provided in [8]. Sort this set based on the total weight in ascending order.
  - After the first metric, use the LIGHTER tool to generate a good estimate in GE.

Finally, we choose the decomposition with a trade-off between minimum total ANF weight and minimum total GE.

The finally chosen  $G(X)$  and  $F(X)$  satisfying all the three TI requirements - Correctness, Non-Completeness and Uniformity are shown in Table II. The chosen  $G(X)$  belongs to  $Q_{293}$  quadratic class and  $F(X)$  belongs to  $Q_{294}$  class [24]. The ANFs

TABLE II  
GIFT S-BOX DECOMPOSITION

$\mathbf{x}$	0	1	2	3	4	5	6	7	8	9	a	b	c	d	e	f
$\mathbf{G}(\mathbf{x})$	4	d	f	7	1	a	2	8	5	c	e	6	0	b	3	9
$\mathbf{F}(\mathbf{x})$	5	6	3	8	1	2	7	c	9	e	f	0	d	a	b	4

for both the quadratic functions are as below:

$$\begin{aligned}
 G(d, c, b, a) &= (g_3, g_2, g_1, g_0) \\
 g_0 &= a + b + ba + c + d \\
 g_1 &= b + ca \\
 g_2 &= 1 + c \\
 g_3 &= a + b + cb
 \end{aligned}$$

$$\begin{aligned}
 F(d, c, b, a) &= (f_3, f_2, f_1, f_0) \\
 f_0 &= 1 + a \\
 f_1 &= a + b \\
 f_2 &= 1 + b + c + d + da \\
 f_3 &= ba + d
 \end{aligned}$$

The corresponding ANFs for eight output shares are provided in Appendix A.

**Sharing using Decomposition (combined 3-shares).** In [9], Kutzner et al. proposed a new methodology to implement the threshold countermeasure presented in [8]. The technique is based on optimizing the area requirements for the protected implementation of a non-linear operation using multiplexers. Referring to ANF equations for the chosen  $G(X)$  and  $F(X)$  in Appendix A, one can clearly see that  $G_1$ ,  $G_2$  and  $G_3$  comprise of similar polynomials and only the indices are different. Similarly,  $F_1$ ,  $F_2$  and  $F_3$  share a similar template. The constant terms are handled in the respective  $G(X)$  and  $F(X)$  function. So, instead of using six different ( $8 \times 4$ ) Boolean functions, we use only two functions – one for  $G(X)$  and another for  $F(X)$ .

As shown in Fig. 3, two multiplexers are used to choose the input for the  $G(X)$  Boolean function depending on which part of the secret it is operating on. After that, a de-multiplexer is used to store the result of the  $G(X)$  operation to the requisite register.  $F(X)$  is implemented in a similar manner and the result is stored in the respective output registers  $OS_1$ ,  $OS_2$  and  $OS_3$ . One must note that the intermediate registers  $g_1$ ,  $g_2$ ,  $f_1$ , and  $f_2$  are required to avoid attacks using glitches.

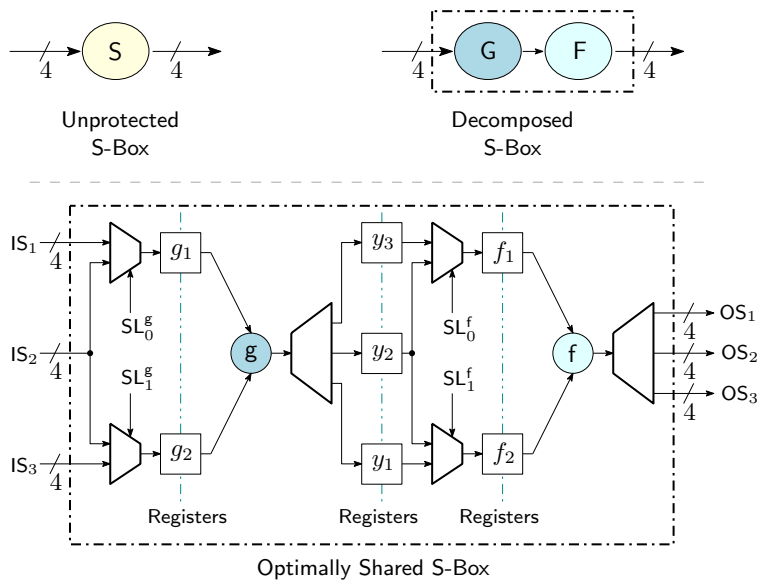


Fig. 3. Sharing using Decomposition (combined 3-shares)

**Direct Sharing (4-shares).** For TI implementation using 4-shares, one uses the minimum required number of shares to share the secret variables. The minimum number of shares  $s$  required to protect a Boolean function from *first-order* DPA attack is given by  $s \geq 1 + d$ , where  $d$  is the algebraic degree of the function [25]. For example, the function  $F(X, Y, Z) = XY + Z$  has an algebraic degree of two. Hence, it requires at least three shares. The ANF equations for the function  $F$  are as stated below:

$$\begin{aligned} F_1 &= Z_2 + X_2Y_2 + X_2Y_3 + X_3Y_2 \\ F_2 &= Z_3 + X_1Y_3 + X_3Y_1 + X_3Y_3 \\ F_3 &= Z_1 + X_1Y_1 + X_1Y_2 + X_2Y_1 \end{aligned}$$

In the case of GIFT, the only non-linear operation is its S-box. The S-box is a  $4 \times 4$  Boolean function (represented as

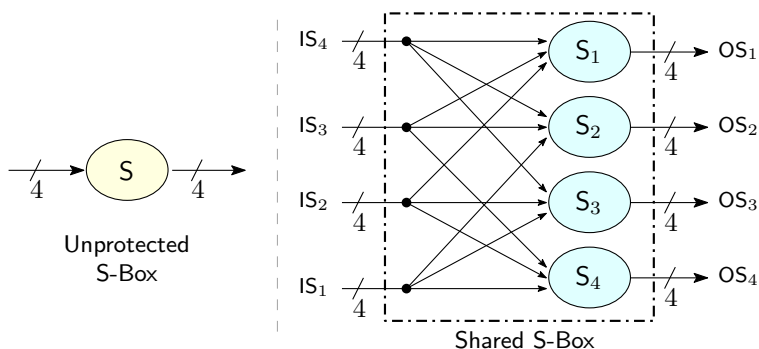


Fig. 4. Direct Sharing (4-shares)

$S(d, c, b, a) \rightarrow (w, z, y, x)$  and has a cubic degree. Hence, we need a minimum of four shares. Fig. 4 shows the approach graphically. The truth table for GIFT S-box is as shown in Table I and its corresponding ANFs are given as:

$$\begin{aligned} S(d, c, b, a) &= (s_3, s_2, s_1, s_0) \\ s_0 &= 1 + a + b + ba + c + d \\ s_1 &= a + ba + c + ca + d \\ s_2 &= b + c + da + db + dc \\ s_3 &= a + db + dca \end{aligned}$$

The output shares ( $OS_1, OS_2, OS_3, OS_4$ ) can be calculated from the above equations. The ANF for the four shares are listed in Appendix B.

An advantage of this technique is that there is no need for additional *registers* in the S-layer. As this approach does not attempt to reduce the degree of the Boolean function before implementation, it results in implementations with significantly large area compared to other techniques.

### B. Implementation Profiles and Their Architecture

Next we present nine different profiles for threshold implementation of GIFT and discuss about various trade-offs. The profiles are a combination of an approach (described in section III-A) with an option. The different options which can be combined with an approach are described as below:

**Option 1:** Sharing of the *data-path*

**Option 2:** Sharing of the *key-register*

**Option 3:** S-box implemented using ANF

**Option 4:** S-box equations optimized using ABC

Since all the profiles are protected, the data-path is shared for all. As shown in Fig. 5, *Profile 1* uses the 3-shares approach

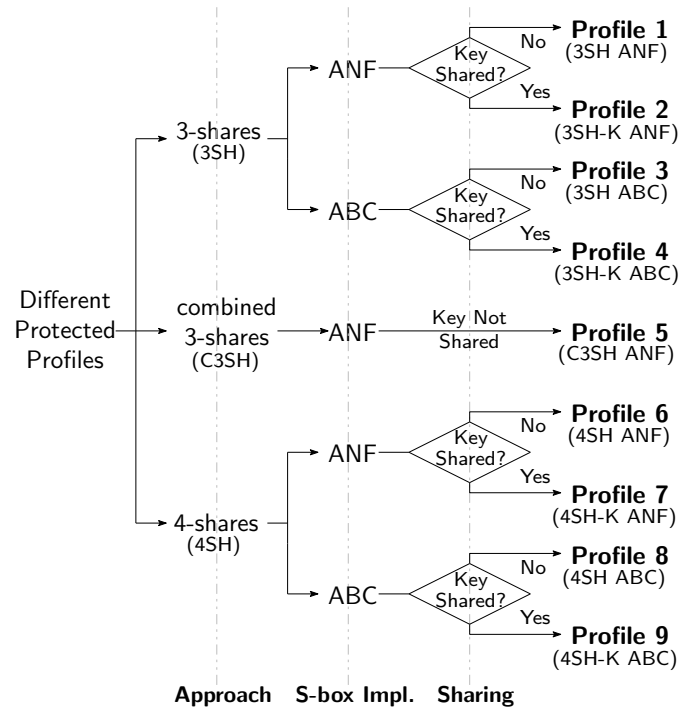


Fig. 5. Different Profiles for Threshold countermeasure

with data sharing and the S-box implemented using ANF representation. *Profile 2* is same as *Profile 1* with an extra shared key register. In *Profile 3*, ABC is used to optimize the S-box. It uses the 3-shares approach with data sharing. Compared to *Profile 3*, *Profile 4* adds sharing of the key register. *Profile 6...9* use same set of options as in *Profile 1...2*, but uses the 4-shares approach. *Profile 5* uses the combined 3-shares approach using multiplexers to switch between the input and output of  $G(X)$  and  $F(X)$ . The data-path is shared in *Profile 5* with ANF representation being used for the S-box implementation. Fig. 6 presents an overall architecture for all the variants of threshold countermeasures we implemented. The solid lines depict

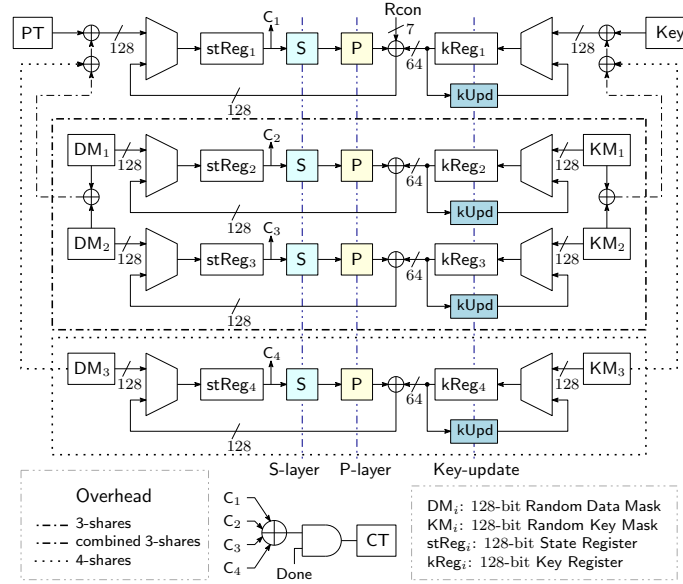


Fig. 6. Overall Architecture for TI techniques for GIFT S-box

the unprotected GIFT implementation. The unprotected implementation comprises of a state-register ( $stReg_1$ ), a key-register ( $kReg_1$ ), a bit-permutation layer and the S-box layer.  $stReg_1$  is used to keep the current state. A multiplexer is used to select between the updated state and the input. The same holds for the  $kReg_1$  key register. The state is updated after applying the S-box, bit-permutation, key and round constant (Rcon) addition steps. For a *parallelized* implementation, one round of unprotected GIFT takes one clock-cycle to update the state-register. So it takes 40 clock cycles to process one block of data.

Additional hardware required for *Profile 1...5* are marked by dashed-dotted regions in Fig. 6. *Profile 1...4* requires two random-mask values ( $DM_1$  and  $DM_2$  128-bit each), two additional state registers ( $stReg_2$  and  $stReg_3$ ), two additional multiplexers, and some XORs. Furthermore, if the key is also shared as in the case for *Profile 2 and 4*, two random-masks ( $KM_1$  and  $KM_2$  128-bit each) for the key, two key registers ( $kReg_2$  and  $kReg_3$ ), and two multiplexers are also required. Implementation of the S-box layer for these profiles depends on whether it is using ANF or ABC, but the overall architecture presented in Fig. 2 remains the same. These profiles also require three additional registers to store the intermediate state in the S-box, hence they take 2 clock-cycles per round of the cipher. As a result, these profiles need 80 clock-cycles in all to process a block. In case of *Profile 5*, the hardware overhead compared to *Profile 1...4* is only in the architecture of the S-box. The S-box in this case is implemented using multiplexers and de-multiplexers as shown in Fig. 3. *Profile 5* requires eight times more clock-cycles compared to the unprotected implementation.

*Profile 6...9* use the 4-shares technique for TI. In this case, in addition to the hardware overheads for 3-shares technique, a random-mask ( $DM_3$ ), a state-register ( $stReg_4$ ) and a multiplexer is required if only the data-path is shared as in the case of *Profile 6 and 8*. *Profile 7 and 9* share both the data-path and the key-register, thus they need an additional random-mask ( $KM_3$ ), a key-register ( $kReg_4$ ), and a multiplexer. The details of the corresponding S-box is shown in Fig. 4. In all of the profiles, the unmasking step is performed by XORing all the respective shares.

### C. Synthesis Results

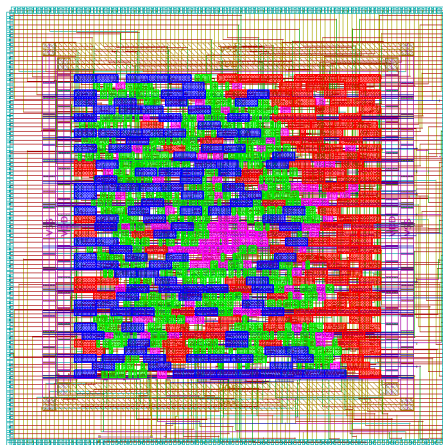
The HDL designs for all of the implementation profiles were written in VHDL<sup>2</sup>. Functional testing was done using the *Xilinx Vivado Simulator* version 2016.3. After functional testing, we used *Synopsys Design Compiler* version J-2014.09 for synthesis of the designs. *Synopsys IC Compiler* version L-2016.03-SP5-1 was used for placement and routing. We used TSMC 65nm Low Power Standard Cell Library (TCBN65LP) for all the ASIC implementations. We used `compile_ultra` during synthesis to get an optimized design. We also used flags to prevent optimization between hierarchal boundaries. *Synopsys PrimeTime* version J-2014.12-SP3-1 was then used on the post-layout design in conjunction with activity factors from simulations done using *Vivado* in order to get accurate power consumption estimates. For this analysis, we focused on getting a balanced design with good area vs. throughput trade-off and hence avoided any specific optimization. This is because aggressive optimization towards area leads to poor timing results and vice versa. It is also important to note that power estimates assume the design running at the highest possible frequency. Running the designs at lower frequency leads to significantly reduced dynamic power consumptions; under such conditions leakage power can be the primary contributor to overall power consumption. The area and power overheads for the random source has not been considered and we assume that the randomness is provided externally.

<sup>2</sup>The HDL files will be available on *github* after the review process.

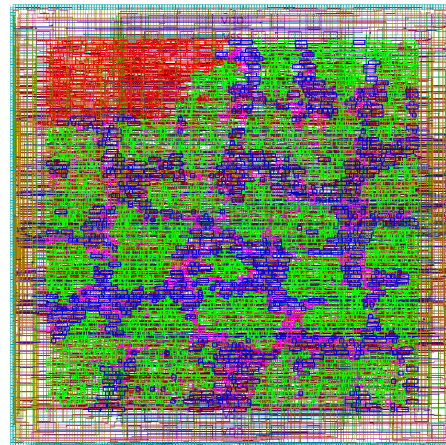
TABLE III  
POST-LAYOUT RESULTS FOR DIFFERENT PROFILES OF THRESHOLD COUNTERMEASURE

Metric	Unprotected		Protected Profiles							
	GIFT	1	2	3	4	5	6	7	8	9
		3SH ANF	3SH-K ANF	3SH ABC	3SH-K ABC	C3SH ANF	4SH ANF	4SH-K ANF	4SH ABC	4SH-K ABC
S-Box Area (GE)	632	7286	7286	7661	7657	2760	18129	18110	84103	84198
State Register Area (GE)	800	3358	3358	3360	3360	8955	3200	3206	3258	3314
Key Register Area (GE)	801	1125	3359	1125	3360	807	801	3200	801	3202
<b>Total Area (GE)</b>	2478	<b>13349</b>	16595	13728	16964	16170	24233	27340	90426	93597
Ratio	1.000	5.387	6.697	5.540	6.846	6.525	9.779	11.033	36.492	37.771
Time (ns)	2.31	2.68	2.71	2.74	2.68	3.9	3.52	3.56	5.56	5.93
<b>Frequency (MHz)</b>	432	373	369	364	373	256	284	280	179	168
# Clock-cycles	40	80	80	80	80	320	40	40	40	40
<b>Throughput (Mbps)</b>	1286	562	556	548	562	97	<b>845</b>	833	532	500
S-Box Power (mW)	0.51	3.01	2.95	3.1	3.13	0.65	5.61	5.52	19.6	18.7
State Register Power (mW)	0.7	2	2.01	2.05	2.13	4.99	3.04	3.1	2.54	2.36
Key Register Power (mW)	0.64	0.72	1.82	0.72	1.81	0.06	0.52	1.62	0.32	1
<b>Total Power (mW)</b>	2.396	7.578	9.217	7.75	9.687	5.8	10.3	11.9	23.8	23.6
<b>Energy (pJ/bit)</b>	1.777	12.859	15.809	13.487	16.438	57.024	<b>11.625</b>	13.624	42.664	45.013
Random bits	0	256	512	256	512	256	384	768	384	768

Fig. 7 shows the *placed* and *routed* physical design for the unprotected, and one of the protected designs. All the protected



(a) Unprotected GIFT, width = 100  $\mu\text{m}$



(b) Protected GIFT (3SH-ANF), width = 200  $\mu\text{m}$

Fig. 7. Two of the *placed* and *routed* designs using *Synopsys IC Compiler*. Colors: S-reg (blue), Slayer (green), Key-reg (red), Glue Logic (magenta)

profiles were compiled using the same script (with different clock constraints). The script was written to accommodate some moderate variations in design complexity.

Table III shows the implementation results for all the profiles. As expected, the protected implementations require more resources than the unprotected one. The smallest protected implementation 3SH is 5.38 times larger. One can see that most of the area is taken up by the S-Box. As direct-sharing leads to very large Boolean equations, the overall area becomes quite large. Depending on the number of shares, key-sharing can triple or quadruple the size of the key-register size. C3SH uses a sequential design as the decomposed S-Box share a similar template. Multiplexers and de-multiplexers are then used



to update the state for all the 3 shares. This leads to a large number of clock cycles and extra intermediate state registers. As the maximum attainable frequency is not too high and the number of parallel operations are reduced (compared to the other designs), the power consumption is the lowest.

It is also interesting to contrast ABC based implementation results with ANF ones. For 3SH the difference is small, whereas for 4SH the difference is quite significant (4.6 times). We believe the reason for this difference is the very large size of expressions in case of direct-sharing. The  $12 \times 4$  mapping in this case leads to about 1100 nodes for one decomposed S-box. Contrasting this with the  $8 \times 4$  mapping used in 3SH which has about 35-55 nodes depending on the specific  $G()$  or  $F()$ , ABC performs significantly better for the latter. As ABC offers many commands and scripts for Boolean-minimization, even with significant effort, reduction in size for very large networks (above 1000 nodes) was about 10 to 30 percent. From these experiments, it is clear that any additional Boolean-minimization is not required as the synthesis tool *Synopsys Design Compiler* was able to perform efficient minimization as it had access to a large library of logic primitives. Fig. 8 shows area

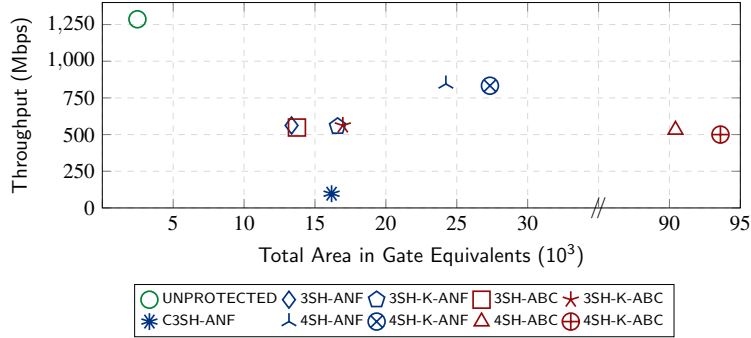


Fig. 8. Area vs. Throughput for all the selected profiles.

vs. throughput for all the profiles. It is evident that 3SH approach leads to smaller area, but as it requires an intermediate register, it ends up taking twice the number of clock cycles. This leads to lower throughput compared to 4SH. As can be seen from Fig. 9, 4SH using ANF consumes less energy even though it has a significantly larger area than 3SH; this can be attributed to its higher throughput. As a result both the designs can be used depending on application requirements. One can also note that the performance and efficiency of C3SH is not good compared to the other designs, so even though it has the lowest power consumption, using such a design is not recommended.

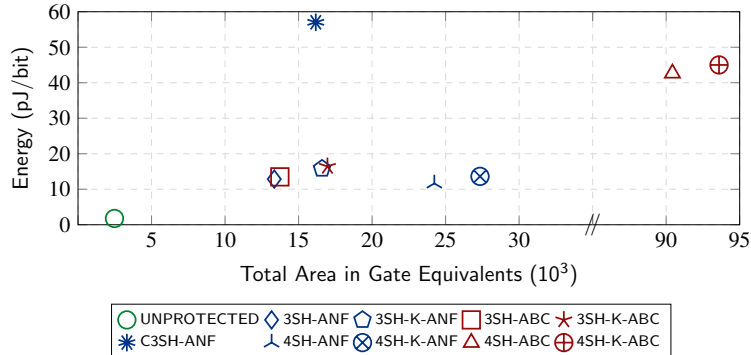


Fig. 9. Area vs. Energy for all the selected profiles.

#### IV. POWER ANALYSIS

In order to evaluate the security of our design, we implemented the design using HDL and tested it on a SAKURA-X board with a Xilinx Kintex-7 XC7K160T FPGA. The power consumption was measured by probing the voltage drop across the 50 milliohms resistor on the 1V0 FPGA core power line. For CPA on the unprotected implementation we used a Tektronix MSO4034 at 2.5 Gs/s and for all TVLA experiments, we used a Teledyne LeCroy HDO6104A at 2.5 Gs/s @ 12 bits/sample. All TVLA experiments were performed using 10 Million traces (5 million traces per set). As the SAKURA-X board is lacking an on-board amplifier we had to use an external preamplifier (Langer 3 Ghz, 30 dB). Considering the small size of GIFT, having a very small leakage signature, it was important to use a pre-amplifier, without it the leakage was below the noise floor and the signal was hardly discernible. In all the experiments, we were running the cipher cores at 48 MHz. The random bits for the masks were generated using AES-128 in counter mode (the operation was interleaved with GIFT).

### A. CPA on the unprotected GIFT cipher

As mentioned earlier, in this paper we only consider round based hardware implementations (FPGA / ASIC), i.e., for every clock-cycle the implementation executes one round or a portion of a round, but, all the plaintext bits and the requisite key bits are processed together. In such implementations, a register is used to store the state and is updated at specific clock events.

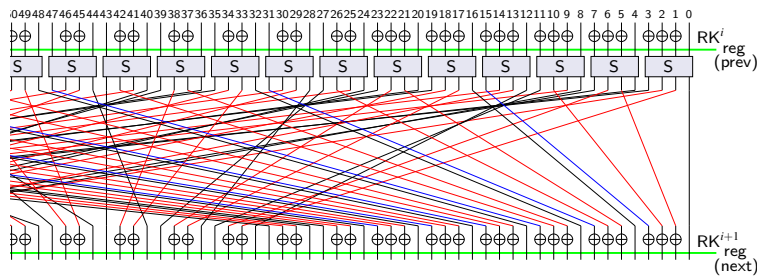


Fig. 10. A portion of the GIFT-128 round function. S is the GIFT S-box and  $RK_i$  is the  $i^{th}$  round-key. The state registers store the value corresponding to the position represented by the green horizontal lines.

Fig. 10 shows the round function of GIFT-128. Assuming an unprotected implementation, the value of the state register is overwritten (updated) at every clock cycle. As a result, the complete cipher execution needs 40 clock cycles (one or two extra clock cycles may be needed for reading in and out the data, depending on implementation). In such implementations, the leakage follows the Hamming Distance (HD) model as the old data in the state register is overwritten by new data which is calculated by combinatorial circuits.

In Fig. 10, value of the register `reg (prev)` is over-written by `reg (next)`. Given the bitwise nature of the permutation layer, for leakage modeling we have to consider one S-box at a time and track which bits are permuted to what locations. Unlike PRESENT, GIFT uses only 64 bits of the round key every round, as a result, for every S-box we can only guess 2 bits; this reduces effectiveness of the CPA attack. Fig. 11 shows two power traces for the reference unprotected implementation of

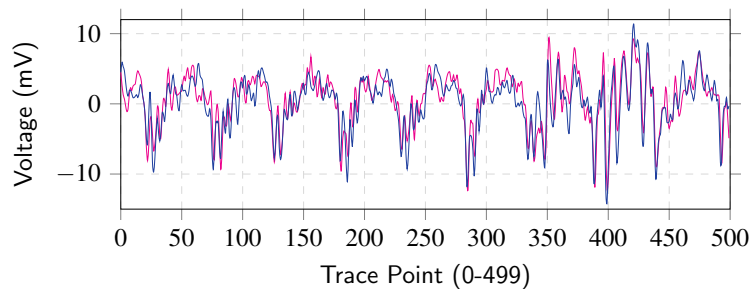


Fig. 11. **Power Trace:** Last 8 rounds of the unprotected GIFT implementation.

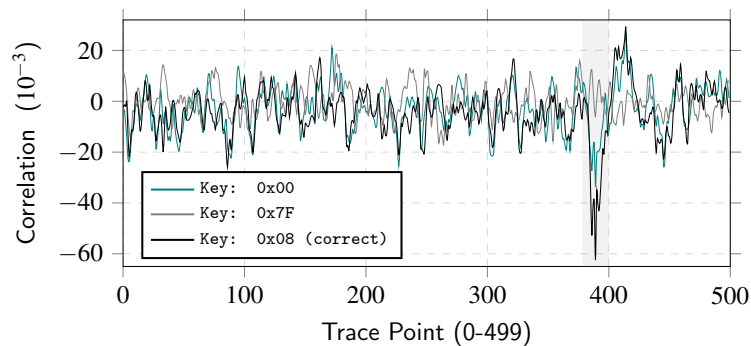


Fig. 12. **Correlation values vs. Trace Point:** For Key Byte 0. A large peak is visible only for the correct key `0x08`.

GIFT. For this attack we try to focus on the last round and try to recover the key used in the last round. We also assume that the cipher-text is known to the attacker; and all the traces use random plain-texts. Considering the first S-box with input bits 0, 1, 2 and 3, according to the permutation, the output bits go to positions 0, 33, 66, and 99 respectively, and then they are XORed with the corresponding round key bits (33 and 66). Bits 0 and 99 pass through unchanged and are known as we

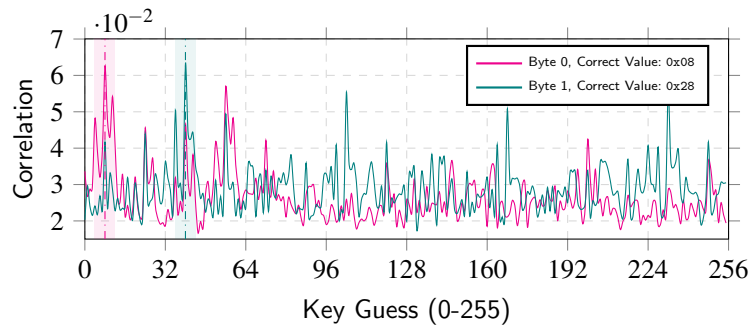


Fig. 13. Correlation values for the two bytes of the key (see text). Peaks at positions 8 and 40 correspond to the correct keys.

know the ciphertext. Now, if we guess two bits of the key (bit 33 and 66 in this case) we can compute the input of the S-box by computing the *inverse* S-box operation. As  $\text{reg}(\text{prev})$  is updated by  $\text{reg}(\text{next})$ , we can now have a valid four bit HD estimate based on a guess of two key bits. This can be used as a hypothetical power model. For the ease of implementation we decided to guess 8 bits of the round-key at a time, as a result we had to process 4 S-boxes at a time. In the rest of the paper, guessing a byte of the key refers to guessing 8 bits which can be in different positions at the last XOR, but arise from a set of 4 S-boxes. Fig. 12 shows the correlation values for three guessed key bytes vs *trace points*. Considering CPA for a successful attack, the correct key has the highest correlation value across the trace points. The peak in the figure for key  $0 \times 08$  corresponds to the time instant at which maximum correlation with leaked key was found. This is the same location of the last round execution as per Fig. 11.

In order to extract the complete round key, we repeated the the above steps for the other 8 bytes and recovered 64 bits. Fig. 13 shows correlation values for all guesses for the first 2 bytes of the last round key. In order to recover the complete key, we have to use the fact that we know the last round-key and go one step back and recover rest of the words of the key. This is possible as the key-schedule uses only rotates and no other function.

### B. TVLA on the protected GIFT cipher

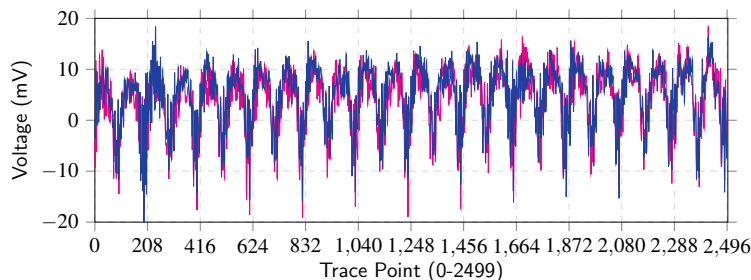


Fig. 14. **Power Trace for 3SH:** Last 10 rounds of the protected GIFT implementation sampled at 5Gs/s. The alternating big and small spikes correspond to the *state update* and the *intra S-box register update* respectively.

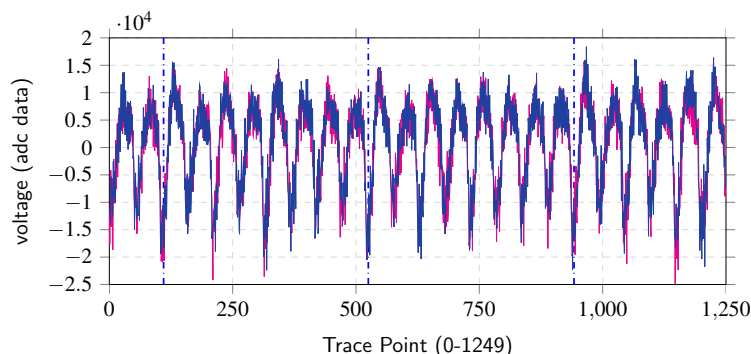


Fig. 15. **Power Trace for C3SH:** Last 2 rounds of the protected GIFT implementation sampled at 2.5Gs/s.

We performed Test Vector Leakage Analysis (TVLA [14]) to evaluate our implementation. More specifically, we used the *specific t-test* leakage detection methodology. For all the experiments, we targeted the last round input-output XOR differences.

The 3SH implementation as mentioned in the previous section uses two registers and 80 clock cycles for 40 rounds. Within a round, the first clock-cycle is used to evaluate the  $G$  function and the second clock-cycle computes  $F$ , the *permutation*, *Rcon-update* and *key-update*. This causes the two clock cycles to consume different amounts of power; this is quite clear in the *power trace* shown in Fig. 14. The C3SH implementation takes 320 clock-cycles for 40 rounds as it uses many intermediate register stages and multiplexers. The power trace for it is shown in Fig. 15.

It is evident from Figure 16 and 17, both the implementations are secure against first order power attacks as the maximum *t-test* value for both the implementations do not reach the chosen threshold. The value of  $\pm 4.5$  is selected based on [14] (which corresponds to a 99.999% probability that the null hypothesis is false for large samples).

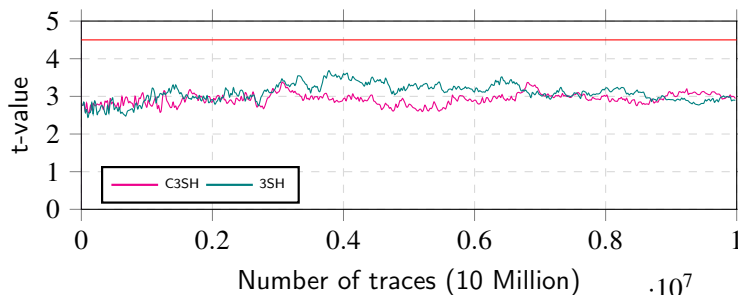


Fig. 16. **TVLA on protected implementations:** TVLA on two of the protected implementations(3SH and C3SH) using 10 million traces. The data points are the *max* of absolute value of the *t-values* for each of the 128-bits. The horizontal red line corresponds to the  $+4.5$  threshold value.

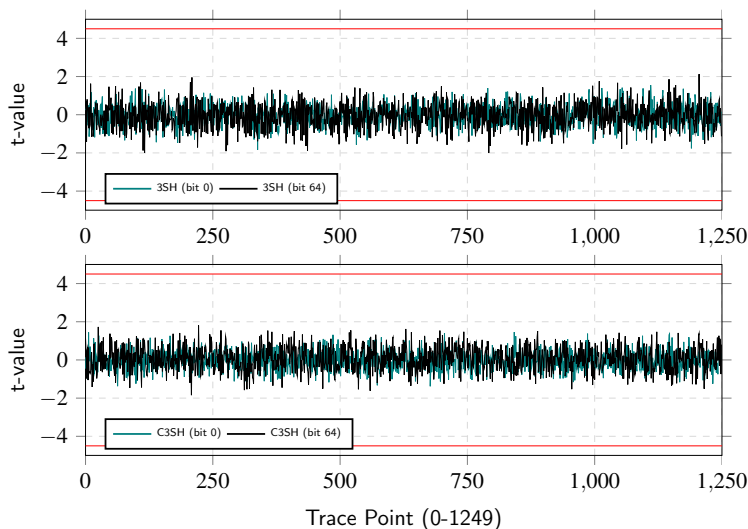


Fig. 17. **TVLA on protected implementations:** Specific *t-test* results for two of the 128-bits for 3SH and C3SH using 10 million traces. The horizontal red lines corresponds to the  $\pm 4.5$  threshold value.

## V. CONCLUSION

In this work, we presented a Correlation Power Analysis attack on the cipher GIFT. We also performed TVLA on two of the protected implementations and showed that they are secure against first-order power attacks. We support this claim by analyzing 10 million traces collected from the respective protected FPGA implementations. Furthermore, we performed design analysis over nine different strategies and give trade-off results for area vs throughput (Fig. 8) and area vs energy (Fig. 9). All the required hardware implementation results are reported in Table III. It is interesting to note certain facts from the presented results:

- 1) Even though 3-shares consumes less power (7.5mW) than 4-shares (10.3mW), the overall energy requirements for the two is comparable as the latter requires only 40 clock-cycles, half compared to the former. So, in a way, a design which consumes more power but finishes earlier can have a lower overall energy consumption.
- 2) Considering throughput vs. area; it is recommended to use 4-shares where higher throughput is required, whereas using the 3-shares will be a good option in constrained environments with less area and moderate throughput.

- 3) The combined 3-shares technique consumes the least amount of power compared to other approaches. But, its throughput is the lowest as well as energy requirements are significantly higher. Hence, using such a design is not recommended for round-based implementations as most of the expected reduction in area is nullified by the large multiplexers and extra intermediate registers (this is not a problem in serialized implementations).
- 4) ANF based implementations takes less area, consumes less power and provides higher or similar throughput as compared to the ones using any Boolean minimization tools, this is especially true when the network is quite large.

In this work we targeted high performance round based implementations, but most of the previous TI implementations focus on serialized implementation to reduce the area. Analyzing such implementations can be a possible future extension.

#### APPENDIX A ANF EQUATIONS FOR 3-SHARES

$$G_1(a_2, b_2, c_2, d_2, a_3, b_3, c_3, d_3) = (g_{13}, g_{12}, g_{11}, g_{10})$$

$$g_{10} = a_2 + b_2 + c_2 + d_2 + a_2b_2 + a_2b_3 + a_3b_2$$

$$g_{11} = b_2 + a_2c_2 + a_2c_3 + a_3c_2$$

$$g_{12} = 1 + c_2$$

$$g_{13} = a_2 + b_2 + b_2c_2 + b_2c_3 + b_3c_2$$

$$G_2(a_1, b_1, c_1, d_1, a_3, b_3, c_3, d_3) = (g_{23}, g_{22}, g_{21}, g_{20})$$

$$g_{20} = a_3 + b_3 + c_3 + d_3 + a_1b_3 + a_3b_1 + a_3b_3$$

$$g_{21} = b_3 + a_1c_3 + a_3c_1 + a_3c_3$$

$$g_{22} = c_3$$

$$g_{23} = a_3 + b_3 + b_1c_3 + b_3c_1 + b_3c_3$$

$$G_3(a_1, b_1, c_1, d_1, a_2, b_2, c_2, d_2) = (g_{33}, g_{32}, g_{31}, g_{30})$$

$$g_{30} = a_1 + b_1 + c_1 + d_1 + a_1b_1 + a_1b_2 + a_2b_1$$

$$g_{31} = b_1 + a_1c_1 + a_1c_2 + a_2c_1$$

$$g_{32} = c_1$$

$$g_{33} = a_1 + b_1 + b_1c_1 + b_1c_2 + b_2c_1$$

$$F_1(a_2, b_2, c_2, d_2, a_3, b_3, c_3, d_3) = (f_{13}, f_{12}, f_{11}, f_{10})$$

$$f_1 = 1 + a_2$$

$$f_{11} = a_2 + b_2$$

$$f_{12} = 1 + b_2 + c_2 + d_2 + a_2d_2 + a_2d_3 + a_3d_2$$

$$f_{13} = d_2 + a_2b_2 + a_2b_3 + a_3b_2$$

$$F_2(a_1, b_1, c_1, d_1, a_3, b_3, c_3, d_3) = (f_{23}, f_{22}, f_{21}, f_{20})$$

$$f_{20} = a_3$$

$$f_{21} = a_3 + b_3$$

$$f_{22} = b_3 + c_3 + d_3 + a_1d_3 + a_3d_1 + a_3d_3$$

$$f_{23} = d_3 + a_1b_3 + a_3b_1 + a_3b_3$$

$$F_3(a_1, b_1, c_1, d_1, a_2, b_2, c_2, d_2) = (f_{33}, f_{32}, f_{31}, f_{30})$$

$$f_{30} = a_1$$

$$f_{31} = a_1 + b_1$$

$$f_{32} = b_1 + c_1 + d_1 + a_1d_1 + a_1d_2 + a_2d_1$$

$$f_{33} = d_1 + a_1b_1 + a_1b_2 + a_2b_1$$

APPENDIX B  
ANF EQUATIONS FOR 4-SHARES

$$S_1(a_2, b_2, c_2, d_2, a_3, b_3, c_3, d_3, a_4, b_4, c_4, d_4) = (s_{13}, s_{12}, s_{11}, s_{10})$$

$$\begin{aligned} s_{10} &= 1 + a_2 + b_2 + c_2 + d_2 + a_2b_2 + a_2b_3 + a_2b_4 + a_4b_3 \\ s_{11} &= a_2 + c_2 + d_2 + a_2b_2 + a_2b_3 + a_2b_4 + a_4b_3 + a_2c_2 \\ &\quad + a_2c_3 + a_2c_4 + a_4c_3 \\ s_{12} &= b_2 + c_2 + a_2d_2 + a_2d_3 + a_2d_4 + b_2d_2 + b_2d_3 + b_2d_4 \\ &\quad + a_4d_3 + b_4d_3 + b_2c_2d_2 + b_2c_3d_2 + b_2c_4d_2 + b_3c_4d_2 \\ &\quad + b_4c_3d_2 + b_2c_2d_3 + b_2c_3d_3 + b_2c_4d_3 + b_4c_2d_3 \\ &\quad + b_4c_3d_3 + b_4c_4d_3 + b_2c_2d_4 + b_2c_3d_4 + b_2c_4d_4 \\ &\quad + b_3c_2d_4 + b_4c_3d_4 \\ s_{13} &= a_2 + b_2d_2 + b_2d_3 + b_2d_4 + b_4d_3 + a_2c_2d_2 + a_2c_3d_2 \\ &\quad + a_2c_4d_2 + a_3c_4d_2 + a_4c_3d_2 + a_2c_2d_3 + a_2c_3d_3 \\ &\quad + a_2c_4d_3 + a_4c_2d_3 + a_4c_3d_3 + a_4c_4d_3 + a_2c_2d_4 \\ &\quad + a_2c_3d_4 + a_2c_4d_4 + a_3c_2d_4 + a_4c_3d_4 \end{aligned}$$

$$S_2(a_1, b_1, c_1, d_1, a_3, b_3, c_3, d_3, a_4, b_4, c_4, d_4) = (s_{23}, s_{22}, s_{21}, s_{20})$$

$$\begin{aligned} s_{20} &= a_3 + b_3 + c_3 + d_3 + a_3b_3 + a_3b_4 + a_3b_1 + a_1b_4 \\ s_{21} &= a_3 + c_3 + d_3 + a_3b_3 + a_3b_4 + a_3b_1 + a_1b_4 + a_3c_3 \\ &\quad + a_3c_4 + a_3c_1 + a_1c_4 \\ s_{22} &= b_3 + c_3 + a_3d_3 + a_3d_4 + a_3d_1 + b_3d_3 + b_3d_4 + b_3d_1 \\ &\quad + a_1d_4 + b_1d_4 + b_3c_3d_3 + b_3c_4d_3 + b_3c_1d_3 + b_4c_1d_3 \\ &\quad + b_1c_4d_3 + b_3c_3d_4 + b_3c_4d_4 + b_3c_1d_4 + b_1c_3d_4 \\ &\quad + b_1c_4d_4 + b_1c_1d_4 + b_3c_3d_1 + b_3c_4d_1 + b_3c_1d_1 \\ &\quad + b_4c_3d_1 + b_1c_4d_1 \\ s_{23} &= a_3 + b_3d_3 + b_3d_4 + b_3d_1 + b_1d_4 + a_3c_3d_3 + a_3c_4d_3 \\ &\quad + a_3c_1d_3 + a_4c_1d_3 + a_1c_4d_3 + a_3c_3d_4 + a_3c_4d_4 \\ &\quad + a_3c_1d_4 + a_1c_3d_4 + a_1c_4d_4 + a_1c_1d_4 + a_3c_3d_1 \\ &\quad + a_3c_4d_1 + a_3c_1d_1 + a_4c_3d_1 + a_1c_4d_1 \end{aligned}$$

$$S_3(a_1, b_1, c_1, d_1, a_2, b_2, c_2, d_2, a_4, b_4, c_4, d_4) = (s_{33}, s_{32}, s_{31}, s_{30})$$

$$\begin{aligned} s_{30} &= a_4 + b_4 + c_4 + d_4 + a_4b_4 + a_4b_1 + a_4b_2 + a_2b_1 \\ s_{31} &= a_4 + c_4 + d_4 + a_4b_4 + a_4b_1 + a_4b_2 + a_2b_1 + a_4c_4 \\ &\quad + a_4c_1 + a_4c_2 + a_2c_1 \\ s_{32} &= b_4 + c_4 + a_4d_4 + a_4d_1 + a_4d_2 + b_4d_4 + b_4d_1 + b_4d_2 \\ &\quad + a_2d_1 + b_2d_1 + b_4c_4d_4 + b_4c_1d_4 + b_4c_2d_4 + b_1c_2d_4 \\ &\quad + b_2c_1d_4 + b_4c_4d_1 + b_4c_1d_1 + b_4c_2d_1 + b_2c_4d_1 \\ &\quad + b_2c_1d_1 + b_2c_2d_1 + b_4c_4d_2 + b_4c_1d_2 + b_4c_2d_2 \\ &\quad + b_1c_4d_2 + b_2c_1d_2 \\ s_{33} &= a_4 + b_4d_4 + b_4d_1 + b_4d_2 + b_2d_1 + a_4c_4d_4 + a_4c_1d_4 \\ &\quad + a_4c_2d_4 + a_1c_2d_4 + a_2c_1d_4 + a_4c_4d_1 + a_4c_1d_1 \\ &\quad + a_4c_2d_1 + a_2c_4d_1 + a_2c_1d_1 + a_2c_2d_1 + a_4c_4d_2 \\ &\quad + a_4c_1d_2 + a_4c_2d_2 + a_1c_4d_2 + a_2c_1d_2 \end{aligned}$$

$$S_4(a_1, b_1, c_1, d_1, a_2, b_2, c_2, d_2, a_3, b_3, c_3, d_3) = (s_{43}, s_{42}, s_{41}, s_{40})$$

$$\begin{aligned} s_{40} &= a_1 + b_1 + c_1 + d_1 + a_1b_1 + a_1b_2 + a_1b_3 + a_3b_2 \\ s_{41} &= a_1 + c_1 + d_1 + a_1b_1 + a_1b_2 + a_1b_3 + a_3b_2 + a_1c_1 \\ &\quad + a_1c_2 + a_1c_3 + a_3c_2 \\ s_{42} &= b_1 + c_1 + a_1d_1 + a_1d_2 + a_1d_3 + b_1d_1 + b_1d_2 + b_1d_3 \\ &\quad + a_3d_2 + b_3d_2 + b_1c_1d_1 + b_1c_2d_1 + b_1c_3d_1 + b_2c_3d_1 \\ &\quad + b_3c_2d_1 + b_1c_1d_2 + b_1c_2d_2 + b_1c_3d_2 + b_3c_1d_2 \\ &\quad + b_3c_2d_2 + b_3c_3d_2 + b_1c_1d_3 + b_1c_2d_3 + b_1c_3d_3 \\ &\quad + b_2c_1d_3 + b_3c_2d_3 \\ s_{43} &= a_1 + b_1d_1 + b_1d_2 + b_1d_3 + b_3d_2 + a_1c_1d_1 + a_1c_2d_1 \\ &\quad + a_1c_3d_1 + a_2c_3d_1 + a_3c_2d_1 + a_1c_1d_2 + a_1c_2d_2 \\ &\quad + a_1c_3d_2 + a_3c_1d_2 + a_3c_2d_2 + a_3c_3d_2 + a_1c_1d_3 \\ &\quad + a_1c_2d_3 + a_1c_3d_3 + a_2c_1d_3 + a_3c_2d_3 \end{aligned}$$

## REFERENCES

- [1] P. C. Kocher, "Timing attacks on implementations of Diffie-Hellman, RSA, DSS, and other systems," in *Advances in cryptology-CRYPTO'96*. Springer, 1996, pp. 104–113.
- [2] P. Kocher, J. Jaffe, and B. Jun, "Differential Power Analysis," in *Advances in cryptology-CRYPTO'99*. Springer, 1999, pp. 789–789.
- [3] S. Mangard, E. Oswald, and T. Popp, *Power analysis attacks: Revealing the secrets of smart cards*. Springer Science & Business Media, 2008, vol. 31.
- [4] K. Tiri and I. Verbauwhede, "A logic level design methodology for a secure DPA resistant ASIC or FPGA implementation," in *Proceedings of the conference on Design, automation and test in Europe-Volume 1*. IEEE Computer Society, 2004, p. 10246.
- [5] S. Mangard, T. Popp, and B. M. Gammel, "Side-Channel Leakage of Masked CMOS Gates," in *CT-RSA*, vol. 3376. Springer, 2005, pp. 351–365.
- [6] S. Mangard, N. Pramstaller, and E. Oswald, "Successfully attacking masked AES hardware implementations," in *CHES*. Springer, 2005, pp. 157–171.
- [7] S. Nikova, C. Rechberger, and V. Rijmen, "Threshold implementations against side-channel attacks and glitches," in *International Conference on Information and Communications Security*. Springer, 2006, pp. 529–545.
- [8] A. Poschmann, A. Moradi, K. Khoo, C.-W. Lim, H. Wang, and S. Ling, "Side-channel resistant crypto for less than 2,300 GE," *Journal of Cryptology*, vol. 24, no. 2, pp. 322–345, 2011.
- [9] S. Kutzner, P. H. Nguyen, A. Poschmann, and H. Wang, "On 3-share Threshold Implementations for 4-bit S-boxes," in *International Workshop on Constructive Side-Channel Analysis and Secure Design*. Springer, 2013, pp. 99–113.
- [10] B. Bilgin, S. Nikova, V. Nikov, V. Rijmen, and G. Stütz, "Threshold implementations of all  $3 \times 3$  and  $4 \times 4$  S-boxes," in *CHES*. Springer, 2012, pp. 76–91.
- [11] B. Bilgin, B. Gierlichs, S. Nikova, V. Nikov and V. Rijmen, "A more efficient AES threshold implementation," in *Africacrypt*. Springer, 2014, pp. 267–284.
- [12] S. Banik, S. K. Pandey, T. Peyrin, Y. Sasaki, S. M. Sim, and Y. Todo, "GIFT: A Small Present," *CHES*, pp. 25–28, 2017.
- [13] E. Brier, C. Clavier, and F. Olivier, "Correlation power analysis with a leakage model," in *CHES*. Springer, 2004, pp. 16–29.
- [14] G. Becker, J. Cooper, E. DeMulder, G. Goodwill, J. Jaffe, G. Kenworthy, T. Kouzminov, A. Leiserson, M. Marson, P. Rohatgi *et al.*, "Test vector leakage assessment (TVLA) methodology in practice," in *International Cryptographic Module Conference*, vol. 1001, 2013, p. 13.
- [15] R. K. Brayton, G. D. Hachtel, C. McMullen, and A. Sangiovanni-Vincentelli, *Logic minimization algorithms for VLSI synthesis*. Springer Science & Business Media, 1984, vol. 2.
- [16] G. D. Hachtel and F. Somenzi, *Logic synthesis and verification algorithms*. Springer Science & Business Media, 2006.
- [17] J. Hlavička and P. Fišer, "BOOM: a heuristic boolean minimizer," in *Proceedings of the 2001 IEEE/ACM international conference on Computer-aided design*. IEEE Press, 2001, pp. 439–442.
- [18] R. Brayton and A. Mishchenko, "ABC: An academic industrial-strength verification tool," in *Computer Aided Verification*. Springer, 2010, pp. 24–40.
- [19] A. Bogdanov, L. R. Knudsen, G. Leander, C. Paar, A. Poschmann, M. J. Robshaw, Y. Seurin, and C. Vikkelsoe, "PRESENT: An ultra-lightweight block cipher," in *CHES*, vol. 4727. Springer, 2007, pp. 450–466.
- [20] A. Shahverdi, M. Taha, and T. Eisenbarth, "Silent Simon: A threshold implementation under 100 slices," in *Hardware Oriented Security and Trust (HOST), 2015 IEEE International Symposium on*. IEEE, 2015, pp. 1–6.
- [21] B. Bilgin, B. Gierlichs, S. Nikova, V. Nikov, and V. Rijmen, "Higher-order threshold implementations," in *International Conference on the Theory and Application of Cryptology and Information Security*. Springer, 2014, pp. 326–343.
- [22] J. Jean, T. Peyrin, S. M. Sim, and J. Tourteaux, "Optimizing implementations of lightweight building blocks," *IACR Transactions on Symmetric Cryptology*, vol. 2017, no. 4, pp. 130–168, 2017.
- [23] C. Carlet, "Vectorial Boolean functions for cryptography," *Boolean models and methods in mathematics, computer science, and engineering*, vol. 134, pp. 398–469, 2010.
- [24] C. De Canniere, "Analysis and design of symmetric encryption algorithms," *Doctoral Dissertaion, KULeuven*, 2007.
- [25] S. Nikova, V. Rijmen, and M. Schläpfer, "Secure hardware implementation of nonlinear functions in the presence of glitches," *Journal of Cryptology*, vol. 24, no. 2, pp. 292–321, 2011.